Bulletin of the Seismological Society of America, Vol. 96, No. 6, pp. 1–, December 2006, doi: 10.1785/0120060004

First Comparison of Array-Derived Rotational Ground Motions with Direct Ring Laser Measurements

by W. Suryanto, H. Igel, J. Wassermann, A. Cochard, B. Schuberth, D. Vollmer, F. Scherbaum, U. Schreiber, and A. Velikoseltsev

Abstract Recently, ring laser technology has provided the first consistent observations of rotational ground motions around a vertical axis induced by earthquakes. "Consistent," in this context, implies that the observed waveforms and amplitudes are compatible with collocated recordings of translational ground motions. In particular, transverse accelerations should be in phase with rotation rate and their ratio proportional to local horizontal phase velocity assuming plane-wave propagation. The ring laser installed at the Fundamentalstation Wettzell in the Bavarian Forest, Southeast Germany, is recording the rotation rate around a vertical axis, theoretically a linear combination of the space derivatives of the horizontal components of motion. This suggests that, in principle, rotation can be derived from seismic-array experiments by "finite differencing." This has been attempted previously in several studies; however, the accuracy of these observations could never be tested in the absence of direct measurements. We installed a double cross-shaped array of nine stations from December 2003 to March 2004 around the ring laser instrument and observed several large earthquakes on both the ring laser and the seismic array. Here we present for the first time a comparison of array-derived rotations with direct measurements of rotations for ground motions induced by the *M* 6.3 Al Hoceima, Morocco, earthquake of 24 February 2004. With complete 3D synthetic seismograms calculated for this event we show that even low levels of noise may considerably influence the accuracy of the array-derived rotations when the minimum number of required stations (three) is used. Nevertheless, when using all nine stations, the overall fit between direct and array-derived measurements is surprisingly good (maximum correlation coefficient of 0.94).

Introduction

To fully characterize the motion of a deformable body at a given point in the context of infinitesimal deformation, one needs three components of translation, six components of strain, and three components of rotation, a vectorial quantity (e.g., Aki and Richards, 2002). Standard seismometers, however, are designed to only measure the translational components of ground motion. Even though seismologists have pointed out the potential benefits of measuring strain (e.g., Mikumo and Aki, 1964; Smith and Kasahara, 1969; Sacks *et al.*, 1976) and rotational ground motions (Aki and Richards 2002), observations of the latter were not made until quite recently. Nigbor (1994) successfully measured translational and rotational ground motion during an underground chemical explosion experiment at the Nevada Test Site by using a triaxial translational accelerometer and a solid-state rotational velocity sensor. The same type of sensor was used by Takeo (1998) for recording an earthquake swarm on Izu peninsual, Japan. Moriya and Marumo (1998) introduced a rotational sensor consisting of two oppositely oriented seismometers. Teisseyre *et al.* (2003) used a rotational-seismograph system with two oppositely oriented seismometers, having pendulums suspended on a common axis, to record small earthquakes at Ojcow Observatory, Poland, and L'Aquila Observatory, Italy.

However, the resolution of the instruments described previously was too low to be applicable in seismology over a broad magnitude and distance range. Therefore, sensor developments in the past years focused on the refinement of optical instruments, in particular, using laser technology. The application of the Sagnac effect for sensing the inertial rotation by using laser principles was first discussed in the sixties (Post, 1967). Two approaches apply the Sagnac effect for rotational measurements, namely active techniques, as in ring laser gyroscopes, and passive techniques, as in fiber-optic interferometers (Sanders *et al.*, 1981). The first application of a ring laser gyroscope as a rotational sensor in

seismology was reported by Stedman *et al.* (1995). Furthermore, McLeod *et al.* (1998) gave a detailed analysis of observation with the ring laser named CI, installed in the so-called Cashmere cavern, Christchurch, New Zealand. They reported that the phase of rotation determined by CI is consistent with that of a collocated standard seismometer record, during the M_L 5.3 Kaikoura event on 5 September 1996. Pancha *et al.* (2000) analyzed the horizontal and vertical components of teleseismic surface and body waves recorded by larger ring laser gyroscopes (CII and G0) caused by *M* 7.0 and *M* 7.3 events at distances of 31° and 42.6°, respectively. Apart from amplitudes of rotation rates larger than expected, they showed—but only in a narrow frequency band—that the sensors provided sufficient accuracy to record seismic rotations. Fully consistent rotational motions were recorded by a ring laser gyro installed at the Fundamentalstation Wettzell, Germany (Igel *et al.*, 2005). They showed that the rotational motions were compatible with collocated recordings of transverse acceleration by a standard seismometer, both in amplitude and phase. This implies that "standard" rotational sensors with sufficient resolution may be possible in the near future.

The full benefits of the determination of rotational motion in seismology are still under investigation. Rotational motions can provide accurate data for arrival times of *SH* waves and, in the near-source distance range, rotational motions might provide more detailed information on the rupture processes of earthquakes (Takeo and Ito, 1997). Rotational motions could also be used to better estimate the static displacement from seismic recordings, identifying translational signals caused by rotation (Trifunac and Todorovska, 2001). Igel *et al.* (2005) introduced a method to estimate the horizontal-phase velocity by using the ring laser data as well as the transverse acceleration estimated from collocated standard seismographs, whereas the standard procedure to estimate phase velocity is array measurements. Even though the comparison with theoretical predictions of phase velocities looks promising (Igel *et al.*, 2005; Cochard *et al.*, 2006), it remains to be seen whether the estimates are accurate enough. In earthquake engineering, observations of rotational components of seismic strong motions may be of interest as this type of motion may contribute to the response of structures to earthquake-induced ground shaking (Li *et al.*, 2001). Most of rotational/torsional studies of ground motion in earthquake engineering are, so far, still carried out by indirect measurements.

Indirect measurements of rotational motions using a seismo- (accelero-) meter array have been studied by several investigators (e.g., Niazi, 1986; Oliveira and Bolt, 1989; Spudich *et al.*, 1995; Bodin *et al.*, 1997; Singh *et al.*, 1997; Li *et al.*, 2001, Huang, 2003). However, to the best of our knowledge, no comparison of array-derived rotation rate and direct measurement from rotational sensors has been described in the literature to date.

Here, for the first time, we present a comparison of rotational ground motions derived from seismic-array data with those observed directly with a ring laser system. The goal of this study is to discuss the effects of noise and uncertainties in the array observations and their relevance to the derivation of rotation. In an era with more and more array-type experiments and processing, the question of direct versus array-type measurements becomes of interest in seismology, earthquake physics, and geodesy. We first present a synthetic study, in which we investigate the influence of various effects on array-derived rotation rate. These effects are (1) unwanted signals (i.e., noise) in the horizontal components of translation, (2) uncertainty in seismometer calibration, and (3) uncertainty in station coordinates. Finally, we show the direct comparison of the vertical component of array-derived rotation rate with the ring laser gyroscope record for the *M* 6.3 Al Hoceima, Morocco, earthquake of 24 February 2004. We conclude that the fit between these entirely independent measurments of the same wave-field property is surprisingly good.

The Experiment

After the successful observation of fully consistent rotational motions (Igel *et al.*, 2005), a mobile seismic-array experiment with eight stations (S1–S8) was installed around the geodetic station Wettzell, Southeast Germany, the location of the ring laser. A ninth station was located in the geodetic station itself (12°52′44″E, 49°08′39″N), where a broadband seismometer (station WET, part of the German Regional Seismic Network, GRSN) is situated. The ring laser is located approximately 250 m from the broadband seismometer. The radius of the seismic array is about 1.5 km, centered at station WET. The shallow subsurface structure consists of metamorphic rock basement covered by glacial till. The location of the array is shown in Figure 1.

Each seismic station consists of a three-component velocity sensor (Le3D-5s) having a flat response in ground velocity between 0.2 and 40 Hz, and a 400 V/m/sec generator constant. A 24-bit three-channel digital recorder was used to record the data. The sampling rate was 62.5 Hz and Global Positioning System (GPS) time synchronization was achieved every 15 min. The experiment was running from December 2003 until early March 2004. The seismometers were buried in soft forest ground or they were deployed on outcropping large igneous rock boulders. The GRSN (WET) station is equipped with a STS-2 broadband instrument with a response to ground velocity from 8.33 mHz (120 sec) to 50 Hz. The data are recorded with a sampling rate of 80 Hz.

The ring laser instrument, called "G," consists of a He-Ne gas laser with a ultrahigh-vacuum quality cavity enclosing an area of 16 m^2. The vertical component of rotation rate is recorded by this instrument with a sampling rate of 4 Hz. In principle, rotations as small as 10^{-10} rad/sec/$\sqrt{\text{Hz}}$ (Schreiber *et al.*, 2003) can be observed (unfortunately this limit is seldom reached). Further information on the ring laser instrument is given in Schreiber *et al.* (2005). Several teleseismic earthquake events were observed during this ex-

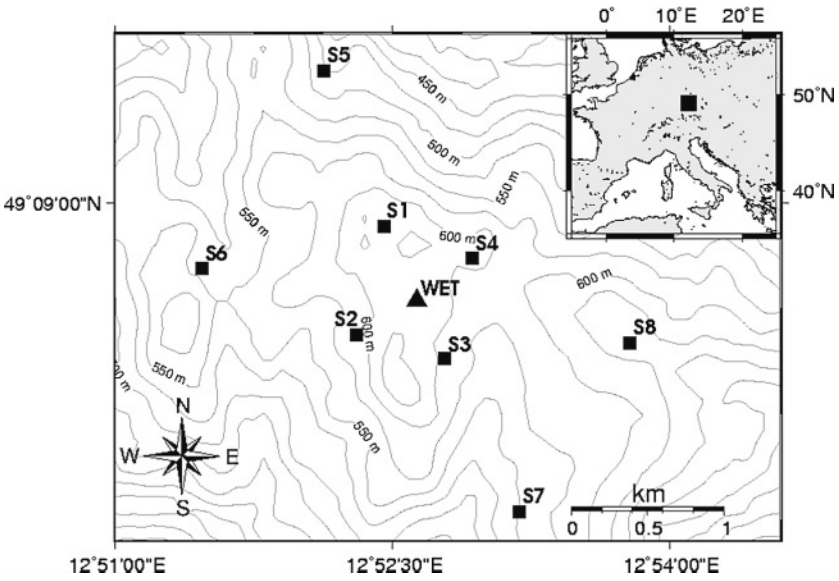

Figure 1. Location of the array experiment. The ring laser and GRSN (German Regional Seismic Network) broadband station (WET) are located at the center of the array marked by a triangle. The ring laser and the broadband seismometer are separated by approximately 250 m.

periment. However, very few of these events were recorded with high signal-to-noise ratio by both the ring laser system and the seismic array. We focus here on the event with the highest signal-to-noise ratio.

Observations and Processing

The earthquake that is investigated occurred on 24 February 2004 at 02:27:46.2 (UTC). The epicenter was near the Mediterranean city of Al Hoceima (35.235° N, 3.963° W) about 295 km northeast from Rabat, Morocco. This earthquake occurred near the eastern end of the Rift mountain belt, which is part of the boundary between the African and Eurasian plates. The distance between the epicenter and the seismic network was about 2055 km (18.5°). This M 6.3 earthquake was recorded simultaneously by array stations S1–S8, the broadband station (WET), and the ring laser. The array and broadband data are corrected for the instrument response and deconvolved to a uniform seismometer with a corner frequency of 0.02 Hz. Figure 2 shows the corrected horizontal components of velocity seismograms, including broadband (WET) data. These components are needed to calculate the horizontal spatial derivatives necessary to estimate the vertical component of rotation rate. All the seismograms, including the broadband data are then bandpass filtered from 0.03 to 0.5 Hz. As expected, after correcting for the instrument response, for an earthquake at such an epicentral distance, considering the frequency band and the size of the array, there is almost perfect match in amplitude and waveform between the array seismograms and the broadband sensor, highlighting the successful correction of the instrument transfer function. The maximum amplitude of the velocity was about 0.8×10^{-4} and 1.2×10^{-4} m/sec for east–west and north–south components, respectively. However, a certain level of noise is visible for some of the stations (e.g., S4, located on an outcropping boulder; and S5, located in very wet forest mud). One of the key questions to be addressed here is how such noise affects the array-derived rotational motions. In the following, we briefly describe how rotation rate can be derived from the horizontal components of array seismograms, and then apply the method to synthetic and observed seismograms.

Deriving Rotation from Seismic-Array Data

The relation between rotational and translational motions is obtained through the application of the curl operator $\nabla\times$ to the seismic wave field v (x, y, z) by:

$$\begin{pmatrix}\omega_x\\ \omega_y\\ \omega_z\end{pmatrix} = \frac{1}{2}\,\nabla \times v = \frac{1}{2}\begin{pmatrix}\partial_x v_z - \partial_z v_y\\ \partial_z v_x - \partial_x v_z\\ \partial_x v_y - \partial_y v_x\end{pmatrix}. \qquad (1)$$

This implies that, in principle, the rotational components can be estimated if we are able to calculate the spatial derivatives of ground velocity. As is well known from numerical mathematics, partial derivatives (in one dimension) can be approximated by introducing information from two or more points sampling the vector field and solving an approximate system of linear equations. In what follows, we restrict ourselves to rotation around a vertical axis, because this is the component the ring laser is measuring. The simplest method to approximate the derivatives of the horizontal components of motion is to subtract two recordings of ground displacement and divide by their distance (finite-difference approximation). This can be done especially when the points are distributed regularly in an ideal cross-shaped array (e.g., Huang, 2003). In this article we apply a standard geodetic method to estimate the static displacement for calculating the space derivatives. This was used previously by Spudich *et al.* (1995) to study the dynamic deformation induced by

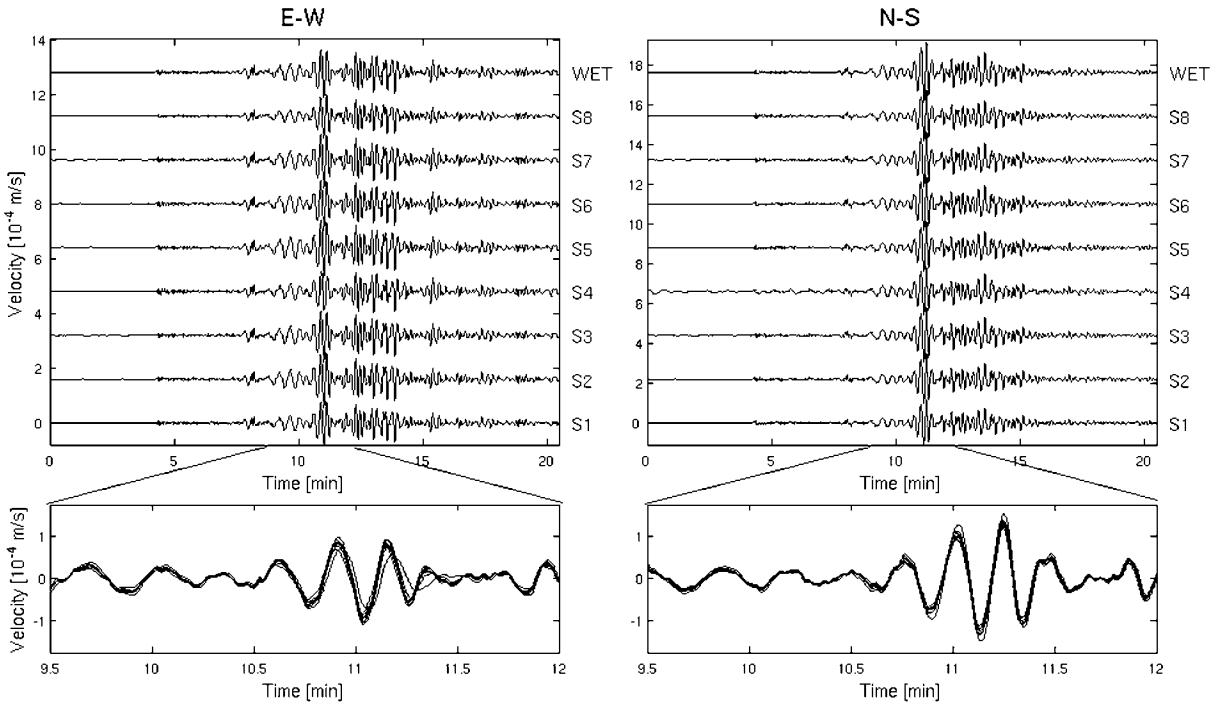

Figure 2. Velocity seismograms for the *M* 6.3 Al Hoceima Morocco earthquake of 24 February 2004 recorded by the array. A superposition of all seismograms in a 2-min time window is shown in the lower part. All seismograms, including the broadband seismogram (WET, top), are corrected for instrument response and bandpass filtered from 0.03 Hz to 0.5 Hz.

the *M* 7.4 Landers earthquake of 28 June 1992, derived from the U.S. Geological Survey Parkfield seismic array (UPSAR) in Parkfield, California. This method was also used by Bodin *et al.* (1997) to study dynamic deformations of shallow sediments in the Mexico basin.

We briefly describe this method in the following. At the free surface boundary, it can be shown that the time-dependent displacement gradient matrix G can be estimated from ground-displacement components u^i ($i = 1 \ldots N$) recorded at N stations by solving the set of equations:

$$d_i = GR_i = \begin{pmatrix} \partial_x u_x & \partial_y u_x & \partial_z u_x \\ \partial_x u_y & \partial_y u_y & \partial_z u_y \\ \partial_x u_z & -\partial_z u_y & -\eta(\partial_x u_x + \partial_y u_y) \end{pmatrix} R_i, \quad (2)$$

where, $\eta = \lambda/(\lambda + 2\mu)$, λ and μ are the Lamé parameters, $d_i = u_i - u_0$, $R_i = r_i - r_0$, u_i, r_i, and u_0, r_0 are the displacements at the coordinates of the ith station and the reference station (subscript 0), respectively. At least three stations must be used to determine the horizontal-displacement gradient using this method.

Assuming the array stations were located at the same elevation, the vertical component of rotation rate ω_z can be obtained by solving equation (2) using three stations (S_i, S_j, S_k):

$$\omega_z = \frac{1}{2A}\left([b_i v_y^i + b_j v_y^i + b_k v_y^k] - [c_i v_x^i + c_j v_x^i + c_k v_x^k]\right), \quad (3)$$

where v^i is the velocity vector at the ith station, A is the area bounded by the station S_i, S_j, and S_k, $b_i = (y_k - y_j)/2$, and $c_i = (x_k - x_j)/2$, and b_j and c_j obtained by index circular permutation. Here, (x_i, y_i), (x_j, y_j), and (x_k, y_k) are coordinates of stations S_i, S_j, and S_k, respectively. When more than three stations are used, equation (2) can be solved using a least-squares procedure. More details can be found in Spudich *et al.* (1995).

Spatial Characteristics of the Seismic-Array Wave Field: Observations versus Simulation

One of the key goals in this study is to understand the effects of various sources of uncertainties in the array observations on the array-derived rotational ground motions. The method described earlier is therefore first tested against a synthetic array data set. Complete theoretical seismograms for translations and rotations were calculated by using a recent 3D global tomography model (Ritsema and Van Heijst, 2000), and a point-source approximation of the Al Hoceima event. Seismograms were calculated using the spectral element method (Komatitsch and Tromp, 2002a,b) that was extended to allow outputting the curl of the velocity-wave

field (i.e., rotation rate). The numerical simulation for this short epicentral distance was carried out with a spatial and temporal resolution allowing an accurate wave field up to periods of 5 sec (Schuberth *et al.*, 2003). The synthetic receivers were located at the same positions as our array seismometers. Figure 3 shows the time histories of the horizontal components of the synthetic ground velocity and superposition of all traces in a short time window. Due to the epicentral distance (~2000 km) and the considered spatial and temporal wavelengths, the waveforms are almost identical across the array. In the following we aim at investigating the effects of noise at some of the seismic stations. As the minimum number of stations to determine the spatial gradient is three, we choose to estimate rotations from triangular (sub-) array sections to investigate (1) the uniformity of the derived rotation across the array and (2) to identify array sections with high noise levels, coupling differences, or instrumental problems. Because of the spatial wavelengths considered in the synthetic wave field, we expect the rotational motions to be close to uniform across the array. Figure 4 shows four pairs of the vertical component of array-derived rotation rate calculated using combinations of three stations of the outermost array stations (S5, S6, S7, and S8) with WET as the reference station (gray line) superimposed with synthetic rotation rate (black line) at the center of the array (WET). The normalized correlation coefficients (maxima) are given above the trace pairs. The stations used to derive the vertical component of the array-derived rotation rate are given in the bottom of each trace pair. As expected with noisefree synthetics, the array-derived rotation rate matches almost exactly the rotation rate calculated at the central station WET (correlation coefficient >0.99).

We now perform the same exercise with the observations of the Al Hoceima event. In Figure 5, the direct observation of rotation rate with the ring laser (black line) at the center of the array is compared with the array-derived rotation rate (gray line) using four different subtriangles. First, we observe that the array-derived rotation rate (using three stations only) varies substantially for the different triangles, suggesting considerable amount of noise, propagation, or site effects across the array. Second, in one subtriangle (S6-WET-S7) the phase match is quite good, but the amplitudes do not match well. In another one (S5-WET-S8) the amplitudes are closer to the direct measurements, but the phases match poorly in most parts of the seismogram. These observations suggest that different sources of noise (amplitude, phase, etc.) seem to affect the various array stations.

Note that here we have deliberately decided to use only three (of nine possible) stations to determine rotations to highlight noise in the data. All stations are used in the final

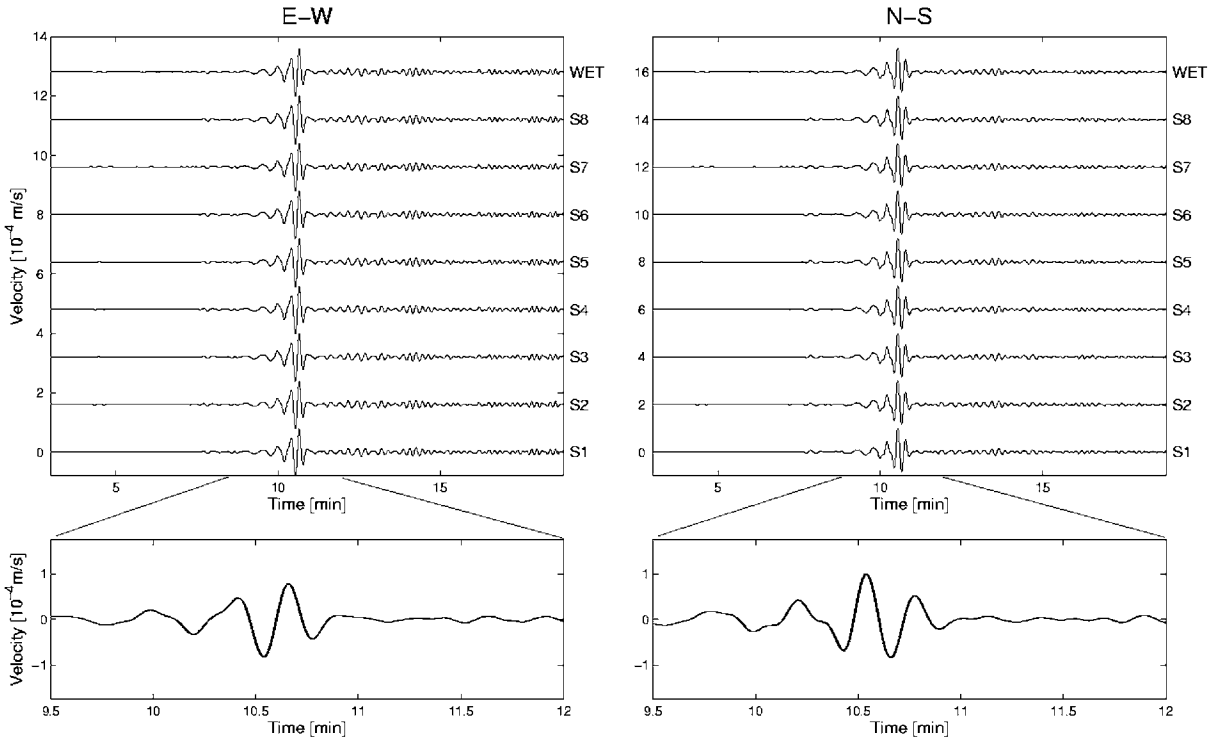

Figure 3. Synthetic velocity seismograms for the *M* 6.3 Al Hoceima Morocco earthquake of 24 February 2004 for all the array stations and the central station (WET), calculated for a 3D mantle model (Ritsema and Van Heijst, 2000) and a recent crustal model (Bassin *et al.*, 2000). The seismograms are calculated using the spectral element method (Komatitsch and Tromp, 2002a,b) and bandpass filtered from 0.03 Hz to 0.5 Hz.

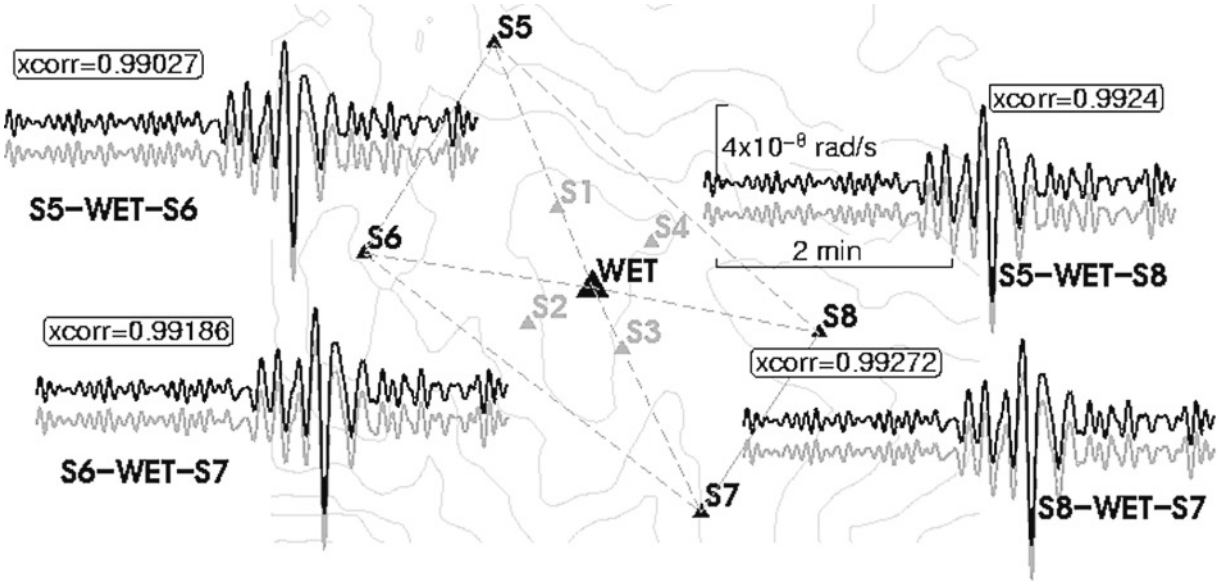

Figure 4. Synthetic test of uniformity of rotation rate across the array. Vertical component of rotation rate at the array center (black lines) and array-derived rotation rate (gray lines) calculated using three stations for four different subtriangles (indicated in each panel). The normalized correlation coefficients are given for each trace pair.

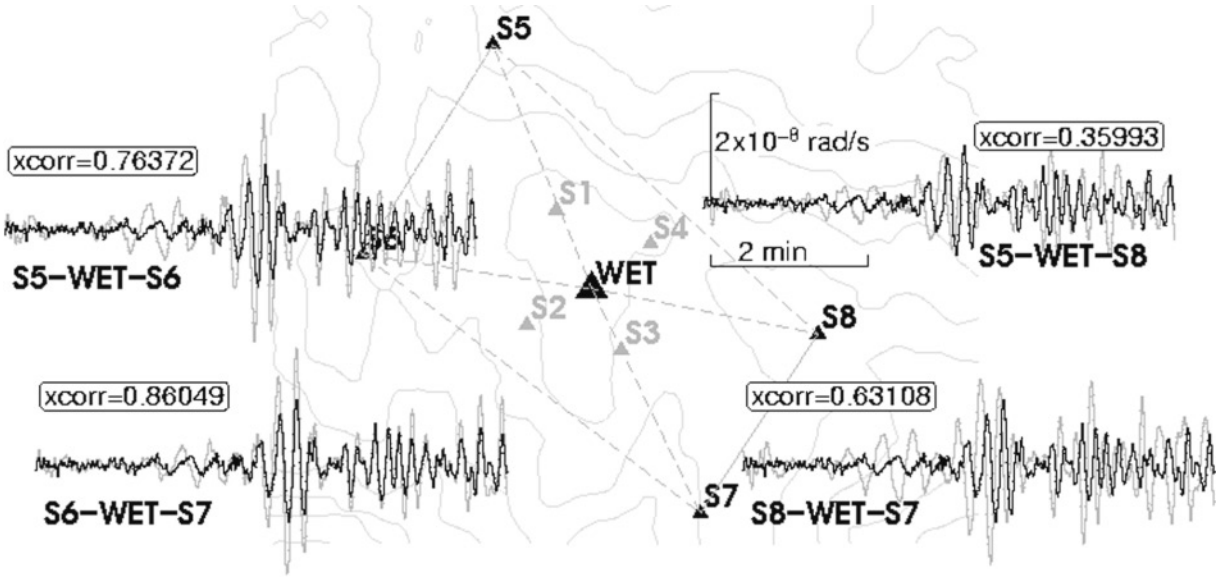

Figure 5. Nonuniformity of array-derived rotation rate (gray lines) across the array in different subtriangles, as noted in each panel, for real data compared with the direct rotational measurements at the center of the array by a ring laser (black lines). The normalized correlation coefficients are given for each trace pair.

comparison. Before investigating specific noise effects more systematically, we demonstrate that, assuming random noise added to the synthetic array seismograms, we reproduce a behavior similar to what is seen in the observations. We add 3% Gaussian white noise to all seismograms. Station 8, however, is additionally altered by phase perturbations in their x and y components. Phase uncertainty is introduced by perturbing each phase component randomly by up to 2% (of 2π). The subtriangle determination of rotation rate with the phase-perturbed synthetics shown in Figure 6a now exhibits misfits similar to those of the observations in Figure 5. The subtriangles containing the phase-perturbed seismometer (S8) compare poorly with the (noise-free) rotational signal at the center of the array. However, if we use all nine stations to determine the rotational signal, most of the random noise cancels out and the final array-derived rotation rate compares

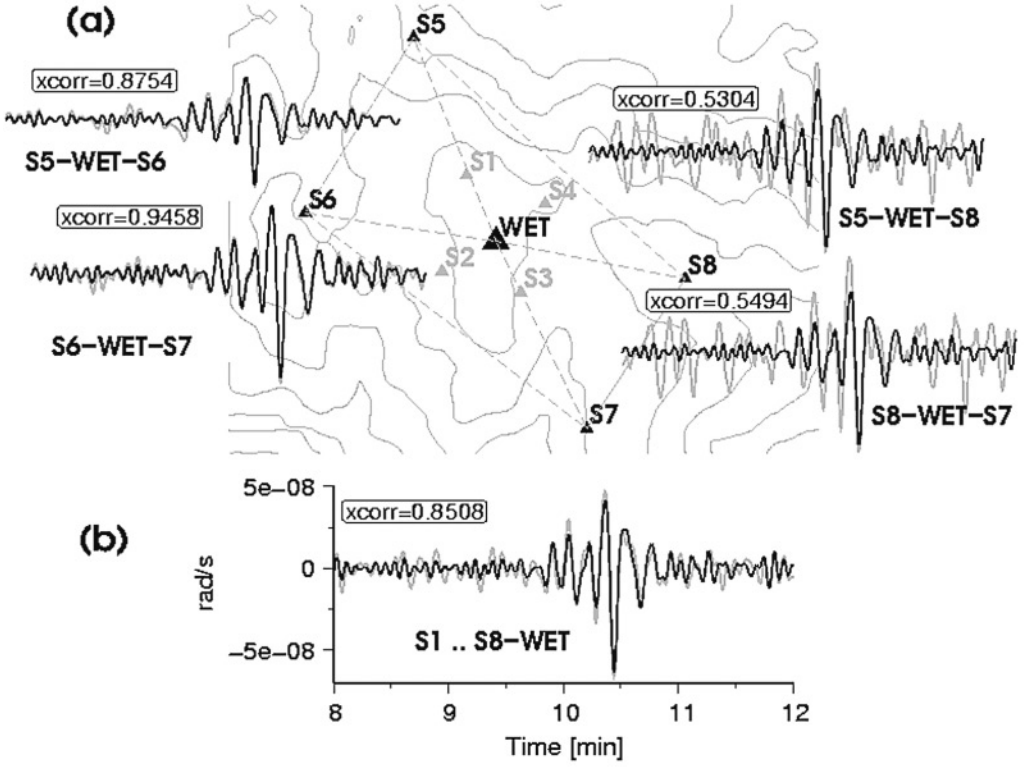

Figure 6. Nonuniformity of array-derived rotation rate across the array for different subtriangles for synthetic data with a single phase-disturbed station (S8, by 2%) and 3% of random noise added for all stations. (a) Vertical component of rotational motions at the center of the array (black lines) superimposed with array-derived rotation rate (gray lines) calculated using three stations, as indicated. (b) Vertical component of array-derived rotation rate (gray) is calculated from all nine stations and compared with the true rotation (black line). The normalized correlation coefficients are given for each trace pair.

well with the (noisefree) rotational signal at the center of the array (Fig. 6b). This indicates that random errors and/or systematic differences (randomly distributed) in parts of the array data may cancel out when a sufficiently large number of stations is used. On the other hand, using only three stations for array-derived rotations may considerably increase the uncertainties with respect to final rotation estimates.

Effects of Noise on Array-Derived Rotations and Comparison with Directly Measured Rotation

In this section we examine the effects of various levels of synthetic uncorrelated random noise, real background noise (extracted from observations), uncertainties in the position determinations, and uncertainties in the seismometer response on the array-derived rotation rate. The vertical component of rotation rate is calculated using all the data from nine stations, as will be done when finally comparing with direct observations. Clearly, intrinsic inhomogeneity of displacement gradients (e.g., due to topography, structural heterogeneity, etc.) might occur, but we restrict ourselves here to the study of random (nonsystematic) perturbations.

To study the effects of uncorrelated random noise in the array seismograms, we generate a Gaussian random signal with maximum amplitudes of 1%, 5%, and 10% of the peak amplitude of the horizontal synthetic velocity seismograms. This random signal is added to the synthetic array data. The array-derived rotation rate from 25 random signal realizations is depicted in Figure 7 (gray) and compared with the noisefree exact rotation rate at the center of the array. The average root-mean-square (rms) difference of the array-derived rotation rate was 1.33%, 6.43%, and 12.87% for 1%, 5%, and 10% noise, respectively. With 10% noise the waveforms are severely distorted but the dominant phases are still well matched with peak amplitude errors similar to the noise percentage. With 5% noise the waveforms are affected by the low-frequency part of the random noise, whereas, with 1%, the differences between the curves are barely visible.

The actual noise level in the observations can be estimated by taking signals prior to the first arriving energy of the event under investigation. In the following, noise signals are extracted from the observations some minutes before the first arriving energy for each of the nine stations. These signals are added to the synthetic array seismograms and the rotational signal is estimated and compared with the noisefree rotational signal at the center of the array. The back-

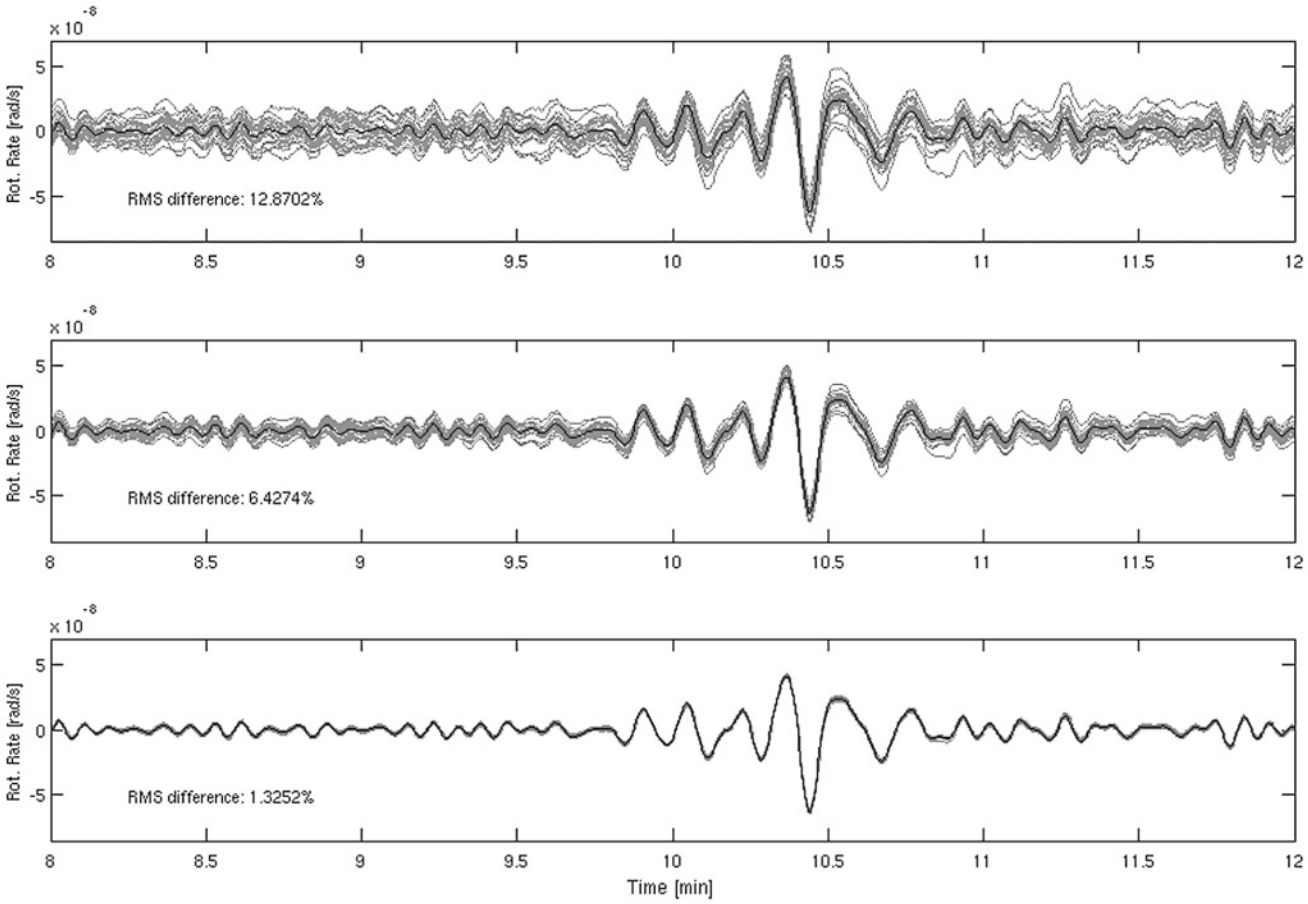

Figure 7. Vertical component of array-derived rotation rate from synthetic data with Gaussian random noise (with 25 noise realizations) (gray line), superimposed with the noisefree synthetic rotation rate (black line). The amount of noise is 10%, 5%, and 1%, from top to bottom. Only for 1% noise is the rotation rate reasonably well retrieved.

ground noise is on average about 3% of the peak amplitude of the velocity seismograms. The results are shown in Figure 8 (top). The rms difference of the array-derived rotation rate with respect to the true signal is 3.58%. These results suggest that with the observed noise level—in the absence of other errors (e.g., systematic errors such as timing, filter problems, etc.)—it should be possible to derive the rotational signal from the array observations with similar certainty (within a few percent).

Array-station coordinates are essential for the calculation of the array-derived rotational signal. In our experiment we use a portable GPS receiver for synchronizing the time and for the determination of the station's coordinates. The problem with this kind of GPS is its low accuracy in position determination. In our experiment, the coordinate precision was affected by the nearby presence of buildings or trees. As a consequence, the uncertainty in seismometer's position in our experiment is several meters. To estimate the effect of position uncertainties, we introduce random position errors from -30 to $+30$ m in the x and y coordinates and calculate the rotation rate for 25 such realizations. The results are shown in Figure 8 (bottom). The average rms difference of the array-derived rotation rate is 0.38%. From this we conclude that the uncertainties introduced through the GPS measurements are unlikely to deteriorate the final array-derived estimates of the rotational signal.

Amplitude errors may be introduced through local site effects at the stations and/or instrumental problems. To investigate the effects we randomly modify the overall amplitude of the synthetic data by a factor of 1%, 5%, and 10%. The calculated rotation rate from 25 realizations in each case is depicted in Figure 9. The rms difference of the array-derived rotation rate is 1.14%, 3.67%, and 10.12%, for 1%, 5%, and 10% amplitude uncertainty in each of the array components, respectively. Even though this test is somewhat simplified, the results suggest that, given our array configuration, random (constant/static) amplitude errors are unlikely to alter the final results significantly,

Array-derived rotation rate is possible under the assumption that the seismometers used in the experiment exhibit the same behavior (i.e., have the same response function). The specific response function of the seismometers used here and the low frequencies considered may potentially introduce phase uncertainties. To investigate this ef-

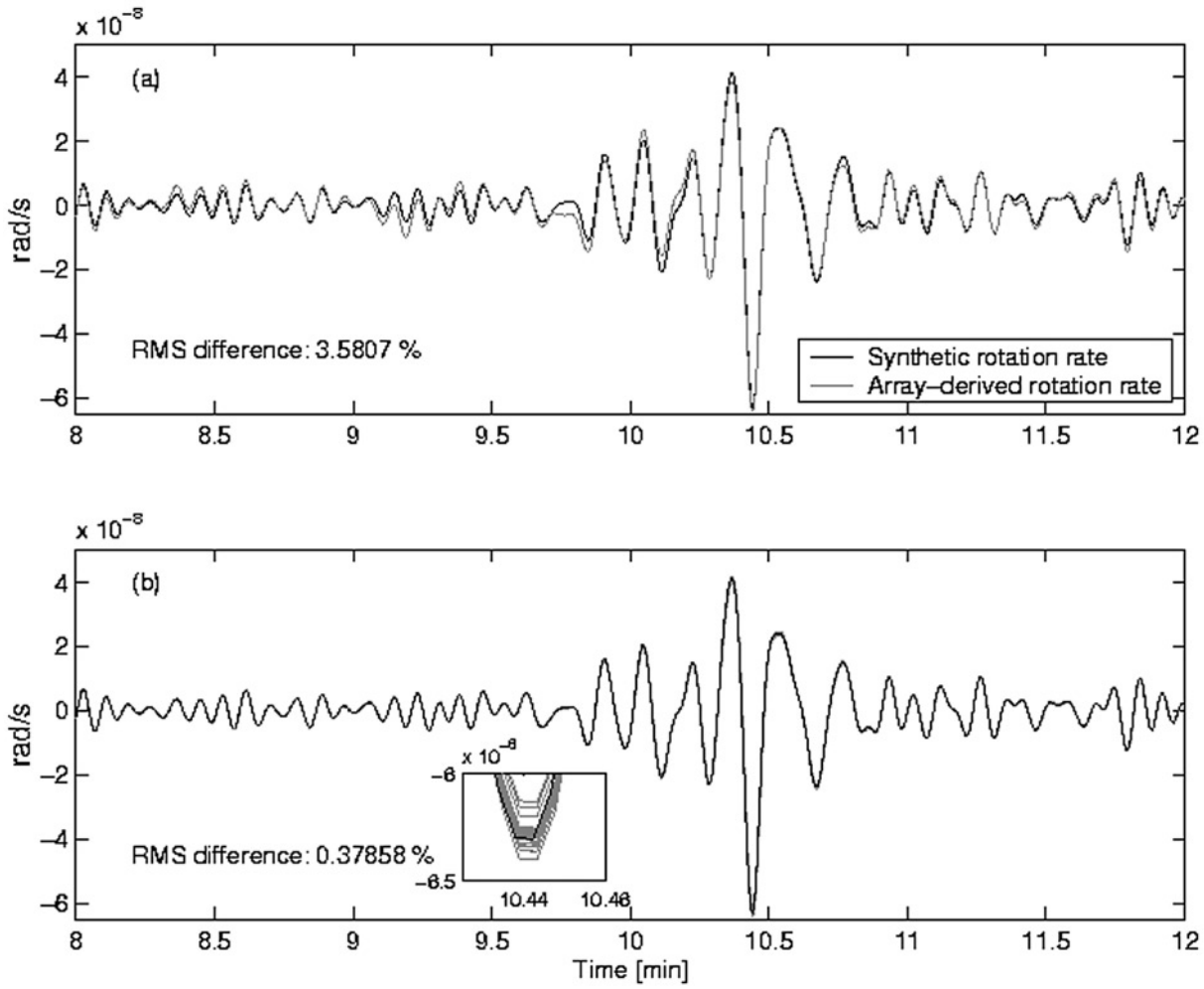

Figure 8. (Top) Vertical component of array-derived rotation rate from synthetic data with real noise taken from the observed seismograms several minutes before the event started. This shows that noise level is not the only cause of the poor results seen in Figure 5. (Bottom) Effects of a ± 30-m maximum error in seismometer position on the derivation of rotation rate for 25 realizations; this shows that inaccuracies in GPS location are unlikely to affect our results.

fect, we alter the phase of all horizontal components in the phase domain by 0.5%, 1%, or 2% (of 2π). The calculated rotation rate from 25 realizations in each case is depicted in Figure 10. The rms difference of the array-derived rotation rate is 65.4%, 38.6%, and 15.5%, for 2%, 1%, and 0.5% phase uncertainty in each of the array components, respectively. Compared with other noise effects, this uncertainty gives the most pronounced effects on the final results. Nevertheless, note that the most dominant phases are still well matched despite the bad overall fit.

Finally, we compute the observed array-derived rotation rate for the Al Hoceima event from the horizontal seismograms of all nine array stations (Fig. 2). In Figure 11 we show the comparison between the array-derived rotation rate with ring laser-based direct measurements of the same wavefield quantity. We stress here that the traces are compared with absolute amplitudes. The overall rms difference is 3.72%. The maximum normalized correlation coefficients are given below each seismogram. The best correlation coefficient is 0.97 in the Love wave-time window. In the early part of the seismogram, the fit is worse. This is probably due to the low amplitudes compared with the peak amplitudes of the Love wave train. In addition, this time window contains the highest frequencies and we expect the uncertainties to increase with frequency because of the finite size of the array. The match between the direct and array-derived rotation rate is almost perfect in the 3-min time window containing the fundamental and higher mode Love waves with correlation coefficients above 0.95. The overall fit worsens toward the end of the signal because of the decreasing signal-to-noise ratio. The surprisingly good fit of those entirely different approaches to measuring the rotational part of the wave field confirms the quantitative results of the synthetic study, in particular the fact that the similarity is obtained

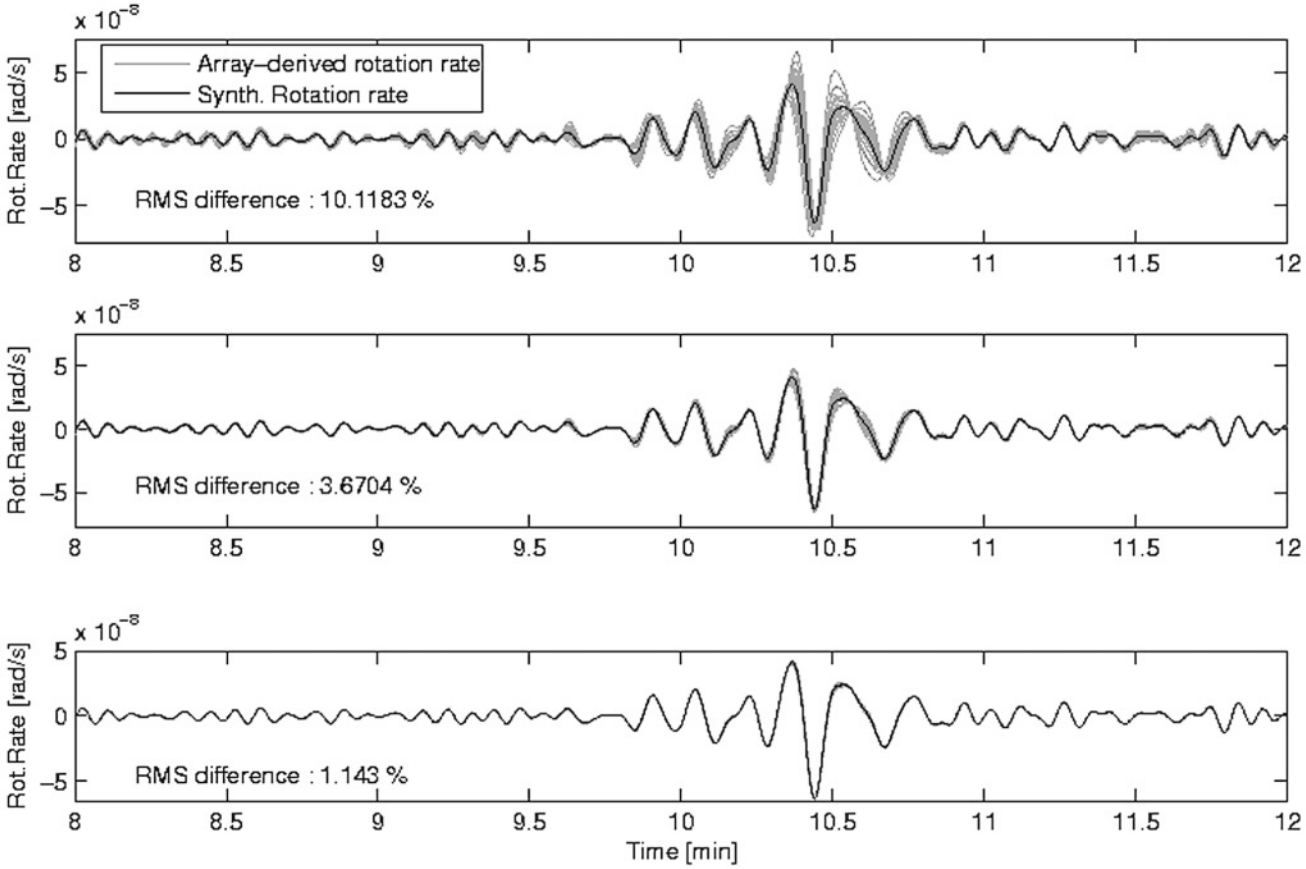

Figure 9. Vertical component of array-derived rotation rate for synthetic data with amplitude uncertainty of 10%, 5%, and 1% (top to bottom), from 25 realizations (gray lines) superimposed with synthetic rotation rate (black line).

thanks to the relatively large number of seismic-array stations given the observed noise levels.

Discussion and Conclusions

Recently, the interest in the observation of rotational ground motions has increased after this type of motion has been neglected for decades, despite the fact that theoreticians suggest it should be observed (e.g., Aki and Richards, 2002). While instruments that directly measure ground rotations are still being developed (e.g., Schreiber *et al.*, 2005), there is more and more evidence that rotational motions may indeed be useful for the understanding of earthquake source processes (Takeo and Ito, 1997), deriving the complete ground motion from rotations and translations (Trifunac and Todorovska, 2001), or in understanding local strong-motion effects due to rotations (Castellani and Zembaty, 1996). Rotational motions can be derived from surface measurements of the horizontal components of at least three stations. This was investigated in several studies (e.g., Bodin *et al.*, 1997; Huang, 2003). However, because at that time appropriate instruments for the direct measurement of rotations were not available, it was impossible to assess the accuracy of these measurements. In the past years, ring laser technology provided the technical means to observe rotational motions around the vertical axis with the required precision in broadband seismology. The full consistency of the ring laser observations with broadband translational motions was shown by Igel *et al.* (2005) and further studies by Cochard *et al.* (2005) and Schreiber *et al.* (2005).

Using ring laser technology we present here the first comparison of seismic array-derived rotations with direct measurements. The goal of this study was (1) to quantify the accuracy with which rotations can be derived from seismic-array data, (2) to investigate the effects of noise, and (3) to discuss issues concerning array versus direct measurements of rotations. The seismic-array experiment that was carried out between December 2003 and March 2004 with a radius of $\approx$1.5 km around the ring laser instrument was to some extent suboptimal because (1) the seismic equipment we used (LE3D-5s) is not designed for long-period signals, and (2) as far as the array geometry goes, the emphasis was on having a shape as close to a regular "finite-difference stencil" as possible, resulting in heterogeneous site conditions (from muddy forest ground to outcropping granite boulders). These conditions and the high noise levels on the horizontal

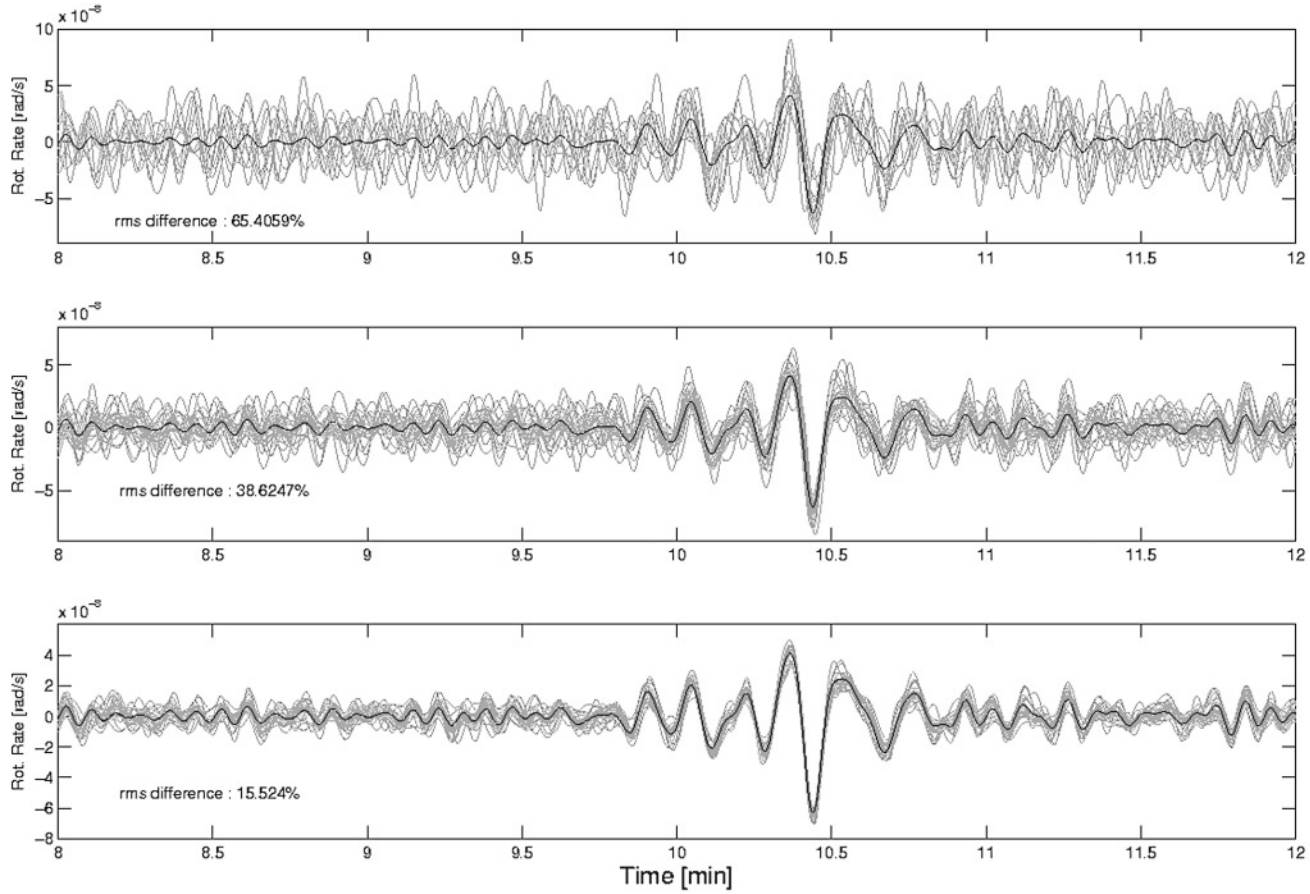

Figure 10. Vertical component of array-derived rotation rate for synthetic data with phase uncertainty of 2%, 1%, and 0.5% (top to bottom), from 25 realizations (gray lines) superimposed with synthetic rotation rate (black line).

components resulted in a data set in which only very few large teleseismic events were usable for the rotation estimates.

Nevertheless, in light of the experimental circumstances the fit between array-derived rotations and direct ring laser measurements (Fig. 11) is stunning, given the observation of a wave-field property (rotation around a vertical axis) with entirely different physical methodologies. We expected that errors in individual station observations would play a stronger role, in particular, when calculating spatial derivatives. The estimated noise level in the array seismograms was about 3%; a quantitatively similar misfit between array-derived rotation and direct measurements is observed for the most dominant signals (Love waves). These results indicate that—given accurate measurements of translational motions in an array of appropriate size and number of stations—the array-derived rotation rate may be very close to the "true" rotational signal that would be measured at the center of the array (or the specific reference station).

However, given the observations described in Figure 5, note that it may be dangerous to use only the minimally required three stations because even relatively small noise levels may deteriorate the rotation estimates. Whereas the results suggest that the observation of array-derived rotations is feasible, note that we considered a fairly long-period signal in this study. Errors will certainly be more pronounced for earthquakes with shorter epicentral distances and higher-frequency wave fields for a given array size. Because of this, the necessity to develop field-deployable rotational sensors with the appropriate resolution for use in local and regional seismology remains an outstanding issue.

Acknowledgments

We thank Jan Hautmann, Markus Treml, Haijiang Wang, Peter Danecek, Julia Linder, and Susanne Lehndorfer for their help, as well as the entire seismology group in Munich University. We also thank the farmers around Wettzell who provided access to their fields throughout the campaign. The idea to carry out this experiment arose over lunch at the DFG Meeting Frauenchiemsee in October 2003. The research was supported by the IQN-Georisk Project (www.iqn-georisk.de), Bundesministerium für Bildung und Forschung (BMBF), and Elitenetzwerk Bayern (International Graduate School, Thesis, http://elite.geophysik.uni-muenchen.de). We thank two anonymous reviewers for their constructive comments.

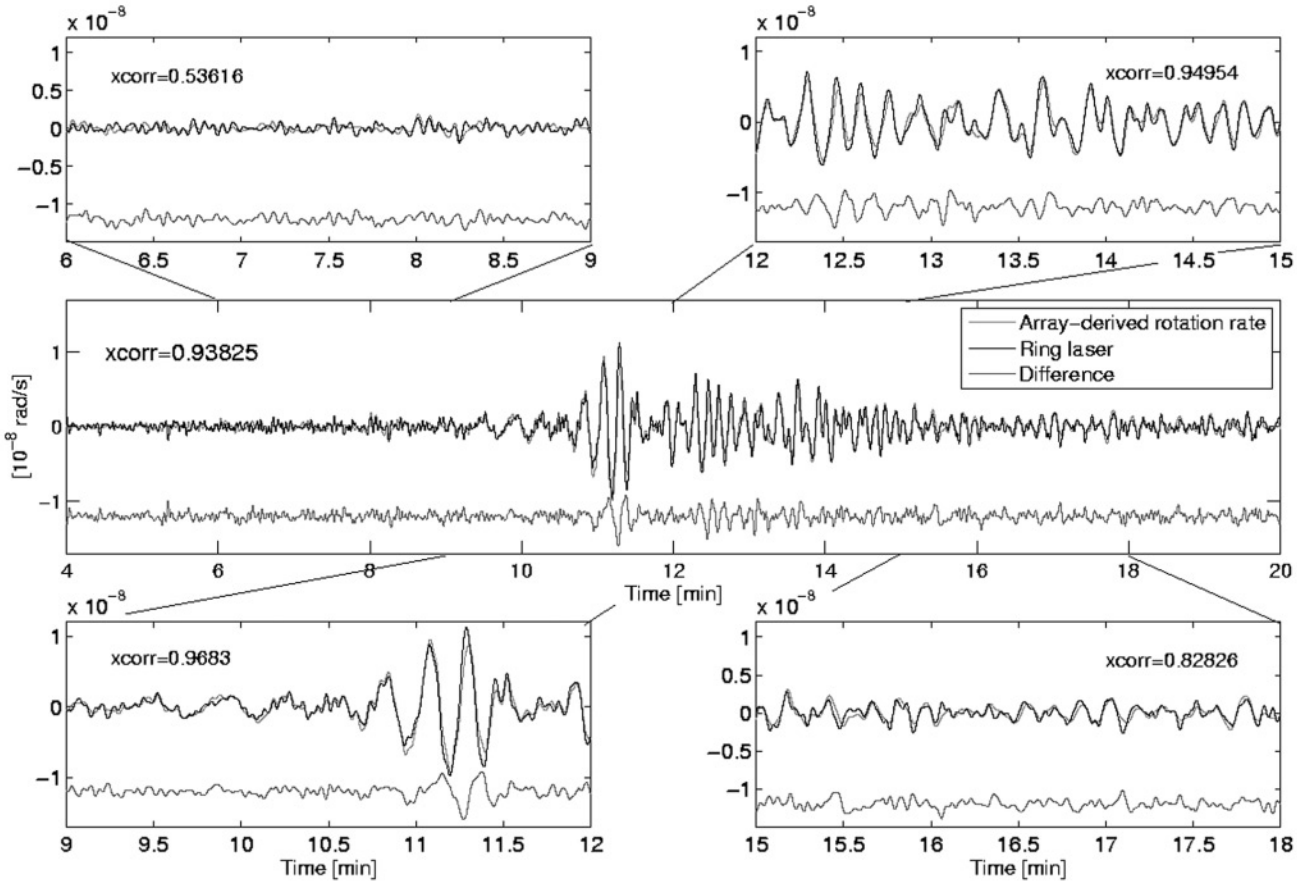

Figure 11. Vertical component of array-derived rotation rate from real array data set (gray line) superimposed with ring laser data (black line), with the difference trace shown below (gray line). Nine stations including the broadband data are used to calculate the array-derived rotational signal. Both traces are bandpass filtered from 0.03 Hz to 0.3 Hz.

References

Aki, K., and P. G. Richards (2002). *Quantitative Seismology*, 2nd Ed., University Science Books.

Bassin, C., G. Laske, and G. Masters (2000). The current limits of resolution for surface wave tomography in North America, *EOS Trans. AGU.* **81,** F987.

Bodin, P., J. Gomberg, S. K. Sing, and M. Santoyo (1997). Dynamic deformations of shallow sediments in the valley of Mexico, Part I: Three-dimensional strains and rotations recorded on a seismic array, *Bull. Seism. Soc. Am.* **87,** 528–539.

Castellani, A., and Z. Zembaty (1996). Comparison between earthquake spectra obtained by different experimental sources, *Eng. Struct.* **18,** 597–603.

Cochard, A., H. Igel, B. Schuberth, W. Suryanto, A. Velikoseltsev, U. Schreiber, J. Wassermann, F. Scherbaum, and D. Vollmer (2006). Rotational motions in seismology: theory, observation, simulation, in *Earthquake Source Asymmetry, Structural Media and Rotation Effects*, D. Teisseyre, *et al.* (Editors), Springer Verlag, New York.

Huang, B. S. (2003). Ground rotational motions of the 1999 Chi-Chi, Taiwan earthquake as inferred from dense array observations, *Geophys. Res. Lett.* **30,** 1307–1310.

Igel, H., U. Schreiber, A. Flaws, B. Schuberth, A. Velikoseltsev, and A. Cochard (2005). Rotational motions induced by the M 8.1 Tokachi-oki earthquake, September 25, 2003, *Geophys. Res. Lett.* **32,** L08309.

Komatitsch, D., and J. Tromp (2002a). Spectral-element simulations of global seismic wave propagation, Part I: Validation, *Geophys. J. Int.* **149,** 390–412.

Komatitsch, D., and J. Tromp (2002b). Spectral-element simulations of global seismic wave propagation, Part II: 3-D models, oceans, rotation, and gravity, *Geophys. J. Int.* **150,** 303–318.

Li, H., L. Sun, and S. Wang (2001). Improved approach for obtaining rotational components of seismic motion, in *Transactions, SMiRT 16*, Washington, D.C., 1–8.

McLeod, D. P., G. E. Stedman, T. H. Webb, and U. Schreiber (1998). Comparison of standard and ring laser rotational seismograms, *Bull. Seism. Soc. Am.* **88,** 1495–1503.

Mikumo, T., and K. Aki (1964). Determination of local phase velocity by intercomparison of seismograms from strain and pendulum instruments, *J. Geophys. Res.* **69,** 721–731.

Moriya, T., and R. Marumo (1998). Design for rotation seismometers and their calibration, *Geophys. Bull. Hokkaido Univ.* **61,** 99–106.

Niazi, N. (1986). Inferred displacements, velocities and rotations of a long rigid foundation located at El Centro differential array site during the 1979 Imperial Valley, California earthquake, *Earthquake Eng. Struct. Dyn.* **14,** 531–542.

Nigbor, R. L. (1994). Six-degree-of-freedom ground-motion measurement, *Bull. Seism. Soc. Am.* **84,** 1665–1669.

Oliveira, C. S., and B. A. Bolt (1989). Rotational components of surface strong ground motion, *Earthquake Eng. Struct. Dyn.* **18,** 517–526.

Pancha, A., T. H. Webb, G. E. Stedman, D. P. McLeod, and K. U. Schreiber (2000). Ring laser detection of rotations from teleseismic waves, *Geophys. Res. Lett.* **27,** 3553–3556.

Post, E. J. (1967). Sagnac effect, *Rev. Mod. Phys.* **39,** 475–493.

Ritsema, J., and H. J. Van Heijst (2000). Seismic imaging of structural heterogeneity in Earth's mantle: evidence for large-scale mantle flow, *Sci. Prog.* **83,** 243–259.

Sacks, I. S., J. A. Snoke, R. Evans, G. King, and J. Beavan (1976). Single-site phase velocity measurements, *Geophys. J. R. Astr. Soc.* **46,** 253–258.

Sanders, G. A., M. G. Prentiss, and S. Ezekiel (1981). Passive ring resonator method for sensitive inertial rotation measurements in geophysical and relativity, *Opt. Lett.* **6,** 569–571.

Schreiber, K. U., H. Igel, A. Cochard, A. Velikoseltsev, A. Flaws, B. Schuberth, W. Drewitz, and F. Müller (2005). The GEOsensor project: rotations—a new observable for seismology, in *Geotechnologies*, F. Rummel, *et al.* (Editors), Springer Verlag, New York

Schreiber, K. U., A. Velikoseltsev, G. E. Stedman, R. B. Hurst, and T. Klügel (2003). New applications of very large ring lasers, in *Symposium Gyro Technology*, H. Sorg (Editor), 8.0–8.7.

Schuberth, B., H. Igel, J. Wassermann, A. Cochard, and K. U. Schreiber (2003). Rotational motion from teleseismic events—modelling and observations (abstract), *EOS Trans. AGU* (Fall Meet. Suppl.), S42D-0200.

Singh, S. K., M. Santoyo, P. Bodin, and J. Gomberg (1997). Dynamic deformations of shallow sediments in the valley of Mexico, part II: Single station estimates, *Bull. Seism. Soc. Am.* **87,** 540–550.

Smith, S. W., and K. Kasahara (1969). Wave and mode separation with strain seismographs, *Bull. Earthquake Res. Inst. Tokyo Univ.* **47,** 831–848.

Spudich, P., L. K. Steck, M. Hellweg, J. B. Fletcher, and L. M. Baker (1995). Transient stresses at Parkfield, California, produced by the M7.4 Landers earthquake of June 28, 1992: Observations from the UPSAR dense seismograph array, *J. Geophys. Res.* **100,** 675–690.

Stedman, G. E., Z. Li, and H. R. Bilger (1995). Sideband analysis and seismic detection in a large ring laser, *Appl. Opt.* **34,** 7390–7396.

Takeo, M. (1998). Ground rotational motions recorded in near-source region of earthquakes, *Geophys. Res. Lett.* **25,** 789–792.

Takeo, M., and H. M. Ito (1997). What can be learned from rotational motions excited by earthquakes? *Geophys. J. Int.* **129,** 319–329.

Teisseyre, R., J. Suchcicki, K. P. Teisseyre, J. Wiszniowski, and P. Palangio (2003). Seismic rotation waves: basic elements of theory and recording, *Ann. Geofis.* **46,** 671–685.

Trifunac, M. D., and M. I. Todorovska (2001). A note on the useable dynamic range of accelerographs recording translation, *Soil Dyn. Earthquake Eng.* **21,** 275–286.

Department of Earth and Environmental Sciences
Geophysics Section
Ludwig-Maximilians-Universität München
Theresienstrasse 41
D-80333 München, Germany
(W.S., H.I., J.W., A.C., B.S.)

Institut für Geowissenschaften
Universität Potsdam
Karl-Liebknecht-Strasse 24/25
14476 Golm, Germany
(D.V., F.S.)

Forschungseinrichtung Satellitengeodäsie
Technical University of Munich
Fundamentalstation Wettzell, Sackenriederstrasse 25
D-93444 Kötzting, Germany
(U.S., A.V.)

Manuscript received 6 January 2006.